Multiferroic BaCoX 2 O 7 (X = P, As) Compounds with Incommensurate Structural Waves but Collinear Spin Ingredients

Bastien Leclercq, Angel Arévalo-López, Houria Kabbour, Sylvie Daviero-Minaud, Alain Pautrat, Tathamay Basu, Claire Colin, Ranjana-Rani Das, Rénald David, Olivier Mentré

Multiferroics $BaCoX_2O_7$ (X = P, As) compounds with incommensurate structural waves but collinear spins ingredients.

Bastien Leclercq [α], Angel M. Arévalo-López [α], Houria Kabbour [α], Sylvie Daviero-Minaud [α], Alain Pautrat [β], Tathamay Basu [β], Claire V. Colin [γ], Ranjana-Rani Das [γ], Rénald David [α], Olivier Mentré[α,*]

[α] Univ. Lille, CNRS, Centrale Lille, Univ. Artois, UMR 8181 – UCCS – Unité de Catalyse et Chimie du Solide, F-59000 Lille, France
[β] Laboratoire CRISTMAT, UMR 6508-CNRS, ENSICAEN, 6 Bd. Du Maréchal Juin, 14000 Caen, France
[γ] Univ. Grenoble Alpes, CNRS, Institut Néel, 38000 Grenoble, France

Abstract: A new paradigm in multiferroics has been observed in $BaCo(X_2O_7)$ (X = As, P) compounds. They consist of 1D-antiferromagnetic chains undulated by incommensurate structural modulations with unusually large atomic displacive waves, giving a mixed 1D/2D "real" magnetic topology. The magnetic ground state is antiferromagnetic (AFM) with k = [½ 0 0] leading to a non-modulated collinear spin-lattice despite the aperiodic atomic framework, and allows developing spin-induced multiferroicity below $T_{N.}$ Severe arguments against the identified mechanisms for type-II multiferroics, *i.e.* by inverse Dzyaloshinskii-Moriya (IDM), exchange striction and spin-dependent *p-d* hybridizations, suggest an original scenario in which the atomic waves, the collinear magnetic structure and magnetic dipole-dipole interactions may interact as crucial ingredients of the spin-induced ferroelectric phase. Here, the specific role of the Co^{2+} spin-orbit coupling (SOC) in the magneto-electric (ME) phase diagram was demonstrated by comparison with the novel Heisenberg $BaFeP_2O_7$ isomorph, similarly structurally modulated. This compound shows a non-collinear modulated AFM ordering, while no ME coupling was detected in its case. Accordingly, both $BaCoX_2O_7$ and $BaFeP_2O_7$ undergo also metamagnetic transitions above 5-6 T promoted by the modulated distribution of spin-exchanges, but the spin-*flop* progressive alignment of the spins in the non-collinear spin-structure (Fe^{2+} case) turns into an abrupt *flip-like* transition in the uniaxial spin-structure (Co^{2+} case).

Introduction: Low Dimensional magnetic materials may provide a platform for developing original multiferroic devices, due to the loss of symmetry elements compared to their 3D-counterpart, often compatible with ferroelectricity [1,2]. From the perspective of fundamental physics, type II multiferroics, are very exciting because one of the orders (generally ferroelectricity) is a consequence of the other (generally antiferromagnetism). Besides their realization in Van der Waals layers or nano-devices, 1D or 2D subunits in bulk materials soften inter-block cohesion and spin interactions, which may reinforce spin-induced polarity in type-II multiferroics (MF), by exchange striction or competing mechanisms. A plethora of arguments for enhanced MF properties in such low-D systems are found in the literature such as i) their predominant insulating behavior necessary for dielectrics [3,4], ii) the persistence of spin ordering in low-D units at relatively high temperature counterpart [5], iii) their good compatibility with the main mechanisms for ferroelectricity of spin origin [6,7], iv) the frustration in low-D topologies playing for spin driven polar atomic shifts [8], v) the possibility of metamagnetic transitions aligning isolated magnetic units with enhanced magneto-electric (ME) exchanges at magnetization steps, see CoV_2O_6 [9,10]. In addition, the effects of magnetic fields on low-D structures open the route to other fascinating phenomena, such as Bose-Einstein condensation or novel field-induced magnetic states such as skyrmions [11]. Here highly anisotropic Co^{2+} spin-chains may generate field-induced particularities, like incommensurate spin density waves (SDW) in the screw AFM chain of $BaCo_2V_2O_8$ [12], metamagnetic *spin-flip* versus *spin-flop* in Co^{2+} chain-systems [13], Spin-dynamics and low-field spin alignments in canted-1D inorganic systems; i.e. $BaCo_2(As_3O_6)_2.(H_2O)_2$[14] analogue to hybrid single-chain-magnets (SCM's) [15,16]. Although ignored up to day, the access to non-collinear magnetic structures and magnetization steps suggest attractive ME properties.

Chemically speaking, most of the low-D cited phases were isolated in BaO-CoO-X_2O_5 systems (X = P, V, As) which highlights the promoting role of large Ba^{2+} cations and XO_4 groups such as phosphates as spacers between low-D subunits [17,18]. The transition metal ion itself dictates the magnetic behaviours through spin orbit coupling (SOC) making the Fe^{2+}, Co^{2+} tandem relevant for contrasted behaviours, see the Ising 2D-ferromagnetic $BaFe(PO_4)_2$ versus quasi-2D XY $Ba(CoAsO_4)_2$ [19,20]. Amongst the variety of reported compounds, $BaCoX_2O_7$ (X = P, As) appear as good candidates for developing spin-induced multiferroicity[21] combining low-D topologies and aperiodic magnetic periods [22,23]. Although the crystal structures reveal spatially isolated AFM-1D chains of ferromagnetic dimers, the existence of metamagnetic M(H) steps around H = 5-6 T questions about the real magnetic topology. In reality, incommensurate structural modulations with unusually strong atomic displacive waves, create undulated 1D-chains which form all together singular quasi 2D layers. Here we propose that the atomic displacive waves assorted with a specific magnetic structure and magnetic dipole-dipole couplings interact as crucial ingredients for an original multiferroic scenario, verified experimentally. In this aim, we have prepared the original $BaFe(P_2O_7)$ isomorph compound for rationalization based on the labile degree of SOC, within an extended series.

$BaFeP_2O_7$ Structural modulation and analogy with the Co^{2+} phases: Polycrystalline samples with single or mixed Fe^{2+}/Co^{2+} cations prepared in the frame of this work are shown in Figure 1a and important notes about the solid state chemistry, synthetic routes and their preliminary physico-chemical characterizations are given in the supplementary, So.

Dealing with the rationalization of magnetic and ME properties of the $BaMX_2O_7$ series, a relevant aspect developed during our work concerns complex spin-lattice coupling within incommensurately modulated materials. The crystal structure of the original $BaFeP_2O_7$ member is modulated similarly to $BaCoX_2O_7$ (X = P, As, V) [21,24]. Its triclinic (S.G. P-*1*, cell parameters *a* = 5.3855(2) Å, *b* = 7.5783(3) Å, *c* = 7.1496(4) Å, α = 102.302(3) °, β = 93.811(3) °, γ = 91.315(3) °) average structure, consists of infinite chains of edge sharing Fe_2O_8 square-pyramid dimers running along the *a*-axis (see Figure 1b), connected by pyro-arsenates As_2O_7 bridges but disconnected in the *ac* plane. These layers are stacked along the *b*-axis and separated by Ba^{2+} cations. Single crystal data show satellites spots fully indexed using the q = [0.16249(3), 0.06573(5), 0.45116(4)] incommensurate modulation vector similarly to the Co and Ni variants [21,24–26].

Its 3D+1 crystal structure was solved in the P-*1(α,β,γ)0* superspace group, after integration of satellites with order up to m = 3. Finally, refining 3rd order displacive waves for all Ba, Fe, P cations and O3 anion and 1st order waves for other oxygen atoms with $R1_{(I > 3\sigma(I))}$ = 5.48 %, see Supplementary Tables 1 for details of the structural refinement (characteristics, positions and thermal displacement). In the same way as the Co^{2+} compounds [21,24] the main atomic displacement occurs along the *c* direction, *i.e.* between individual chains in the *ac* plane, such that the modulated Co-O7 bond distance varies between ~2.2 and ~3.7 Å, locally connecting or not the 1D- chains into 2D-planes[21]. To the best of our knowledge, such "giant" cation-anion modulated separation is uncommon, much above those observed in $(LaS)_{1.196}VS_2$ despite important V-V displacive waves in the latter (~3.05-3.71 Å)[27].

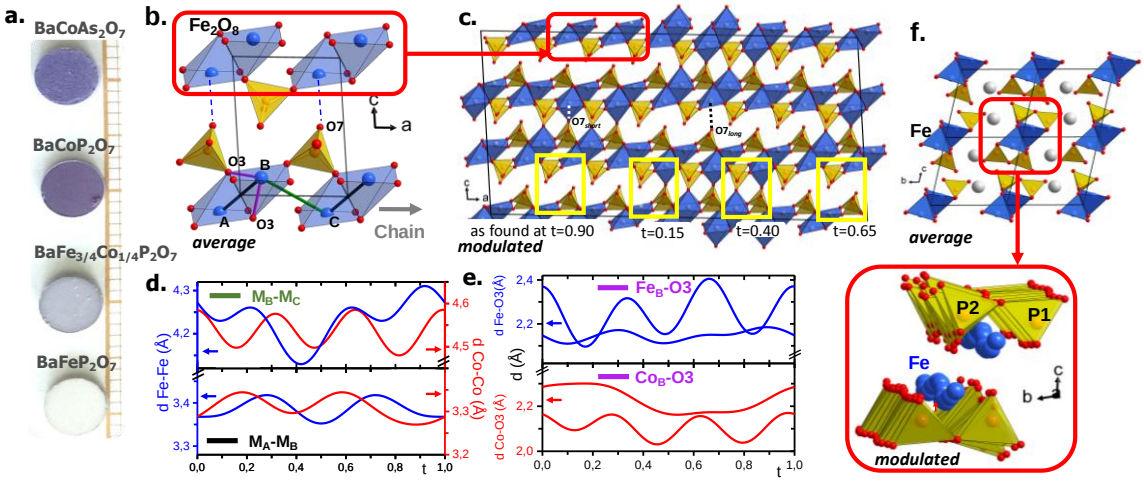

Figure 1 **| *$BaMX_2O_7$ Crystal structure: a)*** *Various $BaMX_2O_7$ (M = Co, Fe, X = P, As) samples and colour changes.* ***b)*** *average unit cell projected along b with with color code for relevant distances.* ***c)*** *7 x 1 x 3 supercell, modulated unit cell with highlight of local structures with Co-Co distances which correspond to the*

average cells at various t as defined in the text. ***d-e)*** *evolution of M_B-M_C, M_A-M_B, Fe_B-$O3$, Co_B-$O3$ distances vs. t.* ***f)*** *average and modulated chains and next As_2O_7 groups along the a-direction.*

Similarly to $BaCoX_2O_7$[21], in $BaFeP_2O_7$ the 3D+1 symmetry strongly affects the connectivity scheme. Between two next layers along *c, it* is mainly anti-phased with those of the next interleave, creating a distribution of compact versus dispersed areas, depending on the strongly modulated Fe--O7 bond distances (~2.3 to 3.7 Å, see S1) within the FeO_{5+1} polyhedra, see Figure 1c. Magnetically, it brings a rare mixed 1D-2D topology. Along the chains axis (*a*-axis), we found that the modulated M-M separation (inside and between the dimers) keep the same amplitude for $BaCoX_2O_7$ and $BaFeP_2O_7$ and can be considered as weak (3.35 to 3.42 Å in the dimers, 4.13 to 4.32 Å between them, see S1) compared to the undulations along the *c*-axis ($d_{Fe\text{-}Fe}$ ~5.4 to 6.3 Å), as plotted along the real space *t*-axis (where t = x4-$\vec{q}.\vec{r}$, $\vec{q}$ is the modulation vector and $\vec{r}$ an average position in physical space) in Figure 1d. On the opposite, the modulated FeO_{5+1} distortion is amplified compared to CoO_{5+1} especially dealing with the M-O3 bonds involved in the shared edge dimeric connection, see Figure 1e. All together, we are dealing with undulated chains of dimers that mainly preserve the Fe-Fe distances "in" and "between" the dimers due to in-phase Fe waves but assorted with strong local distortion of the polyhedra due to the modulated bending of the P_2O_7 groups, see Figure 1f.

Magnetic Properties against cationic specificities : Despite similar incommensurate atomic displacement waves, the magnetic properties of $BaFeP_2O_7$ differ significantly from those of $BaCoX_2O_7$ (X = P, As). The main characteristics of the three key compounds are listed in Table 1. For the three cases, the fundamental state is antiferromagnetic but the magnetic structure and field-dependence differ by contrasted degrees of SOC whose influences on the ME properties are of primary importance. The contrasted θ_{CW} values between the Co^{2+} arsenate (θ_{CW} = -3.75 K) and phosphate (θ_{CW} = -21.7 K) are in good agreement with the hierarchical exchange values latter discussed and the aptitude of PO_4^{3-} oxo-anions for strong magnetic transmission compared to AsO_4^{3-} ones [28,29].

$BaCoX_2O_7$ (X = As and P) shows magnetization plateaus when increasing the applied field assigned to Ms/2[24] or Ms/3 M(H) steps [21] while the saturation is not fully reached at 14 T. In both compounds the rise of the plateaus is abrupt, reminiscent of spin-flip like transitions well supported by Ising Co^{2+} single ions due to the strong SOC, see the μ_{eff} values in Table 1. In fact, our single crystal measurements on $BaCoAs_2O_7$ confirm a broad metamagnetic-like component above 5.5 T especially pronounced along the [100] easy magnetic axis, while a component along the [001] is growing at higher field (*ca.* 9T), see Figure 2a. The sum along the three crystallographic axes creates pseudo-inflexions coincidentally assigned to specific steps. Such pseudo M = M_S/3 magnetic steps were already reported in $(CuBr)Sr_2Nb_3O_{10}$ [30,31].

$BaFeP_2O_7$ is paramagnetic down to *ca.* 20 K and also shows a broad χ(T) maximum at 16.8 K reminiscent of low-D magnetism similar to the Co^{2+} compounds, see Figure 2b. Neel ordering occurs at 10.3 K as confirmed by the heat capacity λ-type anomaly (see Figure 2c,d and Supplementary Figure 2 for extended temperature

range). In contrast, the M(H) magnetization plots differ significantly between Co^{2+} and Fe^{2+} compounds as shown Figure 2b. In the later, M(H) increases progressively even at low field, followed by a smooth metamagnetic transition at 6 T with a rapid increase of the magnetization and weak hysteretic effects between the field increasing and decreasing branches. We observed similar behaviours for Fe/Co solid solution, see Supplementary Figure 3 for the plots and a comparison between pertinent physical parameters. Comparatively to the almost reached saturation in pure Co^{2+} phases, $BaFeP_2O_7$ M(H) barely reaches $3/4^{th}$ of Ms (estimated to 4 μ_B for S = 2 Fe^{2+}) at 14 T which higlight versatile magnetocrystalline anisotropy. Alignment of the powder at 330 K/ 9 T in a gel did not modify the M(H) plot as expected in absence of an easy magnetic axis, see Figure 2b, contrarily to Co^{2+} based series of compounds[24]. This spin flop-like transition suggests Heisenberg isotropic Fe^{2+} individual ions in $BaFeP_2O_7$, in good agreement with the fitted μ_{eff} value of 4.9(1) μ_B/Fe^{2+}, very close to the spin-only moments for S = 2 Fe^{2+} ions (4.89 μ_B) which refute significant SOC contribution, see Table 1, in contrast with the common behavior of Fe^{2+} based oxides [20]. The 3-D Heisenberg character of $BaFe_2P_2O_7$ is comforted by the β critical exponent further refined to 0.36(5) from PND data, in excellent agreement to the 0.367 expected value, Supplementary Figure 4. The situation of $BaFeP_2O_7$ versus $BaCoX_2O_7$ is reminiscent of the recent report of the spin-flop occurring in $BaCo_2As_2O_8.2H_2O$ within a zigzag spin structure versus the spin-flip transition in $Co_2As_2O_7.2H_2O$ with a collinear spin ordering[13]. On this basis, the "flip" versus "flop" like transition types for Co^{2+} and Fe^{2+} respectively suggest uniaxial-collinear spin ordering in $BaCoX_2O_7$ (experimentally verified in [21]) against Heisenberg spins with a plausible non-colinear spin-structure in $BaFeP_2O_7$. Here the softening of a macroscopic easy axis may result from the modulated Fe^{2+} atomic strings and locally modulated FeO_{5+1} distortions along the chains.

The specific heats of $BaCoAs_2O_7$ and $BaFeP_2O_7$ confirm in the former the preservation of the λ-peak at 9 T and highlights a robust/uniaxial AFM state (see Figure 2c,d). Contrarily, in the latter the vanishing of the λ-type into a broad kink at T_N upon increasing the field validates a " forced spin-aligned" state similar to a paramagnet under high field. It resembles the high-field state of $BaCo_2V_2O_8$ in which the field induces an order-disorder transition [12,32,33].

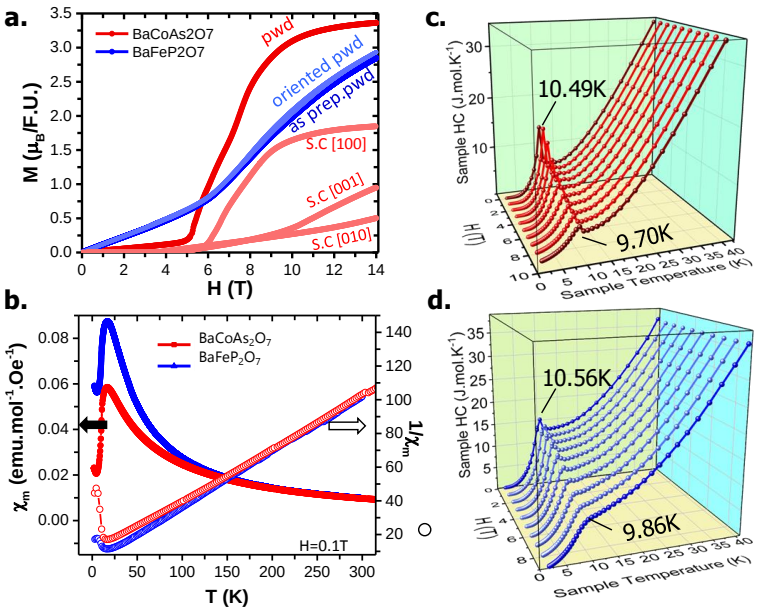

Figure 2 | Magnetic Characterizations a) M(H) plot (2K) for $BaCoAs_2O_7$ (red) and $BaFeP_2O_7$ (blue) powder and single crystal samples (S.C). In the former, the main contribution falls along the a axis, i.e. the chains direction. In the latter, attempts to orientate the powder using eicosane gel at 9 T show the absence of easy magnetic axis. **b)** $\chi_m(T)$ and $1/\chi_m(T)$ plots between 300 and 2 K at 0.1 T. **c)** Specific heat measurement from 0 to 9 T and 40 to 2 K for $BaCoAs_2O_7$, showing the preservation of the T_N-peak. **d)** Same data for $BaFeP_2O_7$, with vanishing of the λ-peak anomaly a T_N into a schottky-like anomaly under field.

Table 1 | Main structural and magnetic features for $BaCoAs_2O_7$, $BaCoP_2O_7$ and $BaFeP_2O_7$ compounds (left to right).

compound	$BaCoAs_2O_7$	$BaCoP_2O_7$	$BaFeP_2O_7$
	Crystallograpy, superspace group P-1(α,β,γ)0		
a (Å), α (°)	5.5386(2), 101.5001(2)	5.3230(6), 101.217(4)	5.3855(2), 102.302(3)
b (Å), β (°)	7.7581(3), 96.4724(2)	7.5799(4), 95.809(8)	7.5783(3), 93.811(3)
c (Å), γ (°)	7.2947(3), 91.6781(2)	7.1174(3), 90.681(8)	7.1496(4), 91.315(3)
Volume ($Å^3$)	304.76(2)	280.09(2)	284.26(2)
q vector	0.13571(4)	0.146(4)	0.1625(1)
	0.0781(1)	0.075(2)	0.0657(1)
	0.4768(1)	0.470(2)	0.4512(1)
	Magnetic Properties		
T_N (K/)	10.68	10.41	10.28
μ_{eff} (μ_B/F.U.)/(calc.)	4.35/3.87	5.1/3.87	4.9/4.89
θ_{CW} (K)	-3.75	-21.7	-10.88
	DFT Calculs (GGA+U average cell) U=4eV Co^{2+} / 6eV Fe^{2+}		
J_{dimer} (K/meV)	+ 2.7/2.3 10^{-2} (FM)	+ 23.1/0.2 (FM)	+1.04/8.9 10^{-3} (FM)
d_{M-M} (Å)	4.53	3.25	3.38
J_{chain} (K/meV)/	- 7.5/-6.4 10^{-2} (AFM) /	-13.1/-0.11 (AFM) /	- 2.8-/2.4 10^{-2} (AFM) /
d_{M-M} (Å)	5.54	5.32	5.38
J_c (K)	- 0.8 / 5.98-6.02	not calc. / 5.86 (2x)	not calc. / 5.79-5.90
J_{dimer}/J_{chain}	- 0.36	-1.76	- 0.37
	Ground State AFM spin Structure (2 K)		
Spins	Collinear non Modul..	Collinear non Modul..	Tilted Modul.

Ref. Moment (μ_B)	3.452(58) total	3.65(12) total	3.3(1) average
$R_{magn.}$ %	6.76	2.09	1.05
Instrument	D2B (ILL), λ=2.4 Å	WISH (ISIS), T.O.F	D1B (ILL), λ=2.52 Å
	Metamagnetism		
H_C (T) (inflexion)	5.14	4.96	6.13
M_{14T} (T)	3.3	3.4	2.9
Allure	Sharp	Sharp	Smooth
Easy magn.axis	[100]	[100]	None
	Magnetic dipole-dipole Interaction		
Jdd $_{dimer}$ (meV)	+ 7.15 x 10^{-3}, repuls.	+ 6.00 x 10^{-3}, repuls.	- 1.01 x 10^{-2}, attract.
Jdd $_{chain}$ (meV)	+ 1.88 x 10^{-3}, repuls	+ 7.21 x 10^{-3}, repuls.	- 1.87 x 10^{-3}, attract.
Jdd $_{dimer}$ total (meV)	+ 7.32 x 10^{-3}, repuls.	+ 6.71 x 10^{-3}, repuls.	- 8.96 x 10^{-3}, attract.
Jdd $_{chain}$ total (meV)	+ 2.36 x 10^{-3}, repuls	+ 6.36 x 10^{-3}, repuls.	- 1.99 x 10^{-3}, attract.
Jdd $_{dimer}$ / Jdd $_{chain}$	3.098	1.055	4.504

AFM ground states *vs.* modulation: The contrasted magnetic responses of the Co^{2+} vs. Fe^{2+} compounds in terms of metamagnetism and degrees of SOC picture different fundamental AFM states at zero field. Indeed, as previously reported, the $BaCo_2P_2O_7$ AFM magnetic ground state is described by a single k = (½ 0 0) propagation vector with respect to a collinear spin structure, Ising compatible [21]. In contrast the isotropic Fe^{2+} single ions in $BaFeP_2O_7$ suggests important spin-lattice coupling and maybe influenced by the structural modulation, as confirmed below. The main phenomena evidenced by PND along temperature and applied fields are shown in Figure 3.

The magnetic structure of $BaCoP_2O_7$ was previously refined ignoring the structural modulation, leading to M_{Co} = 3.730(1) μ_B nearly along the a-axis, *i.e* the chain direction[21]. Dealing with group theory, symmetry mode analysis using Isodistort[34,35] shows that coupling the nuclear incommensurate structural vector with the magnetic X point (½, 0, 0) results in two possible magnetic irreducible representations GP1|mX1+ and GP1|mX1-. The difference between them is an origin shift of the magnetic inversion (1') by 1/4 along the *a* direction. Practically it yields FM dimers AFM coupled (GP1|mX1+) against AFM dimers FM coupled (GP1|mX1-). The refined model clearly validates the former model, in good agreement with the DFT calculated spin exchanges detailed below.

For $BaCoP_2O_7$ (ILL-France, D2b data), NPD refinements converge to M_{Co}= 3.65(12) μ_B similar to the previous report (see Table 1, Figure 4a,d and Supplementary Figure 4). The moments are nearly confined in the (*ab*) planes with the greatest component along *a*, *i.e.* the chain axis. Attempt to affect the magnetic structure using the structural satellites lead to modulated amplitudes smaller than 2σ, see Table 3, leading to a non-modulated picture with AFM chains of collinear and equal FM spin-dimers, along *a*, a non-trivial distribution taking into account the strongly undulated chains.

For $BaCoAs_2O_7$ (ISIS spallation source-UK, WHISH data), the same approach at 0 T results into similar unmodulated spin moment values (M = 3.45(6) μ_B) see Table 3, but one should note a greater M_z component, *i.e.* toward the interchain region (see, Figure 4b,d and also Supplementary Figure 4 for the extended range diagram and details of the refinement). In summary at 0 T for both $BaCoX_2O_7$ materials (X = P, As), FM dimers couple antiferromagnetically mainly along the structural chains, parallel to the *a* direction, see Figure 4a,b. The spins ignore the structural modulation and lie almost confined into the equatorial plane of the CoO_6 octahedra, this reflects the strong Ising-like ion anisotropy of Co^{2+} sensitive to the local orbital overlapping.

For $BaFeP_2O_7$ (ILL, France, D1b data [36]) the situation is quite different, where in addition to the temperature independent structural satellites (q vector), both k_1 = (½ 0 0) AFM satellites and their 1st order satellites modulated by $k_2 = q$ (the structural modulation mode) grow below T_N. The (½, 0, 1)-k_2, (½, -1, 0)-k_2 and (½, 1, 0)+k_2 reflexions show the strongest intensity, see Figure 3b. The average AFM state is similar than for the Co^{2+} materials giving FM dimers AFM coupled along the chains but confined in the (*a,c*) plane this time, i.e. almost normal to the spins in the two Co^{2+} compounds, a direction much more sensitive to the chain undulation. Indeed, the effect of the modulation of the AFM structure with respect to a two k- magnetic structure gives a significant wave component along c, leaving mainly FM dimers with modulated amplitude and directions. The average moment is 3.31(1) μ_B with local values between 2.5-4.2 μ_B, see Figure 4c,d. The spin lattice coupling dictates the spin orientation influenced by the local changes and is responsible for the smooth spin alignment increasing the field, contrarily to the uniaxial Co^{2+} compounds with an abrupt M(H) step. Fitting the $M/M_{max}(T)$ evolution using $A(1-(T/T_N))^{\beta}$ yields β = 0.36(9), as expected for 3-D Heisenberg systems (0.367), see Supplementary Figure 4 (Rietveld refinement plot, non modulated structure representation, and temperature evolution of the refined magnetic moments). The refined moment and wave components of the modulation are listed in Table 2, for the three compounds.

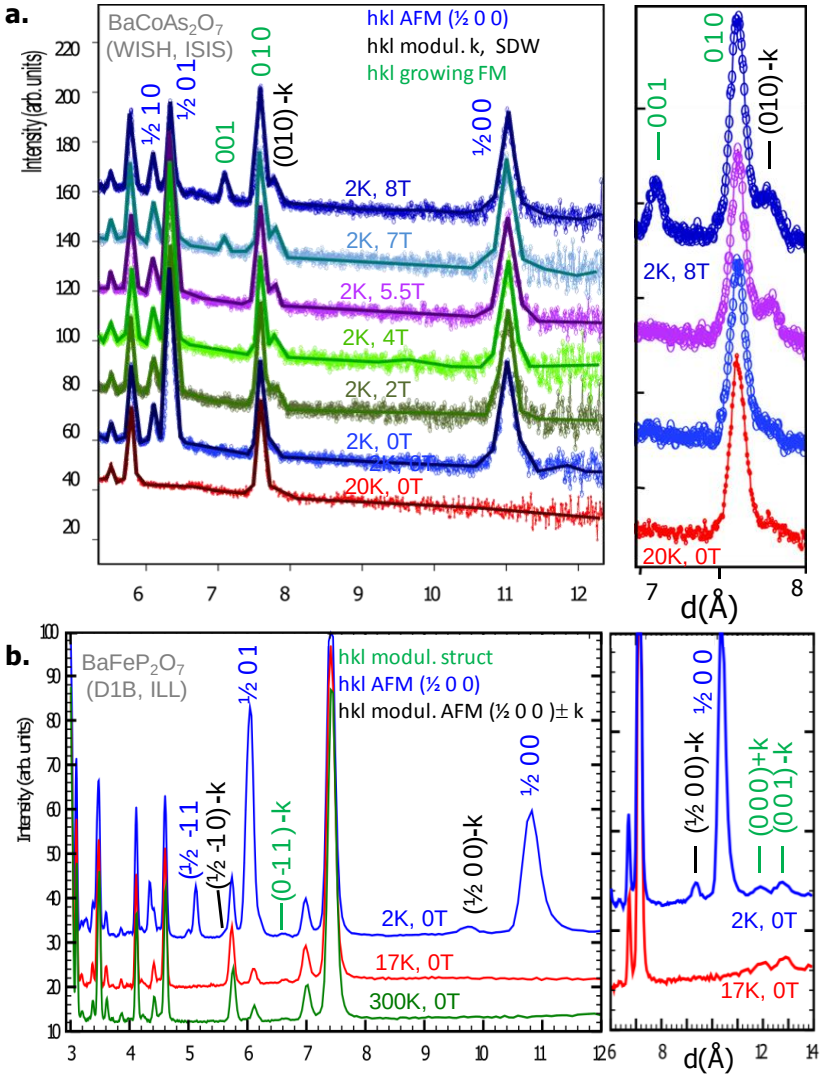

Figure 3 | Powder Neutron Diffraction: **a)** PND patterns for $BaCoAs_2O_7$ of the (WISH, ISIS) from 20 K, 0 T to 2 K, 8 T (bottom up). It shows the k_{AFM} = (½ 0 0) satellites below T_N, the appearing of the incommensurate (k_{SDW} = q) SDW magnetic satellites above 2T and the growing of FM fundamental Bragg components above 7 T. **b)** PND patterns for $BaFeP_2O_7$ (D1b, ILL) versus temperature with highlights of the incommensurate structural (q) peaks in green, the AFM k1 = (½ 0 0) satellites in blue and their 2k modulated satellites by (k2 = q) in black. On the right, enlargement of pertinent areas.

Table 3 **| *Magnetic Modulation*** *refined moments and wave components for $BaMX_2O_7$ compounds using the mixed refinements of the modulated crystal structure and of the modulated AFM spin structure. Only the sinusoidal term along x for $BaFeP_2O_7$ (> 3σ) is significant, as confirmed by the observation of two-k satellites.*

	Atom	Wave	Along a	Along b	Along c	M (μ_B)
$BaFeP_2O_7$	Fe	0	2.69(5)	-0.28(9)	2.02(6)	3.31(12)
		Sin 1	**0.9(2)**	-0.6(3)	0	1.1(4)
		Cos 1	0.3(3)	0	-0.4(2)	0.5(3)
$BaCoP_2O_7$	Co	0	2.92(4)	2.10(4)	0.30(7)	3.8 (1)
		Sin1	0.2(3)	-0.5(3)	0.1(4)	0
		Cos1	-0.2(3)	-0.4(2)	-0.1(4)	0
$BaCoAs_2O_7$	Co	0	3.06(2)	1.79(2)	1.02(4)	3.44 (5)
		Sin1	0.3 (2)	0.0(3)	-0.3(2)	0
		Cos1	0.1 (2)	0.0(3)	0.2(2)	0

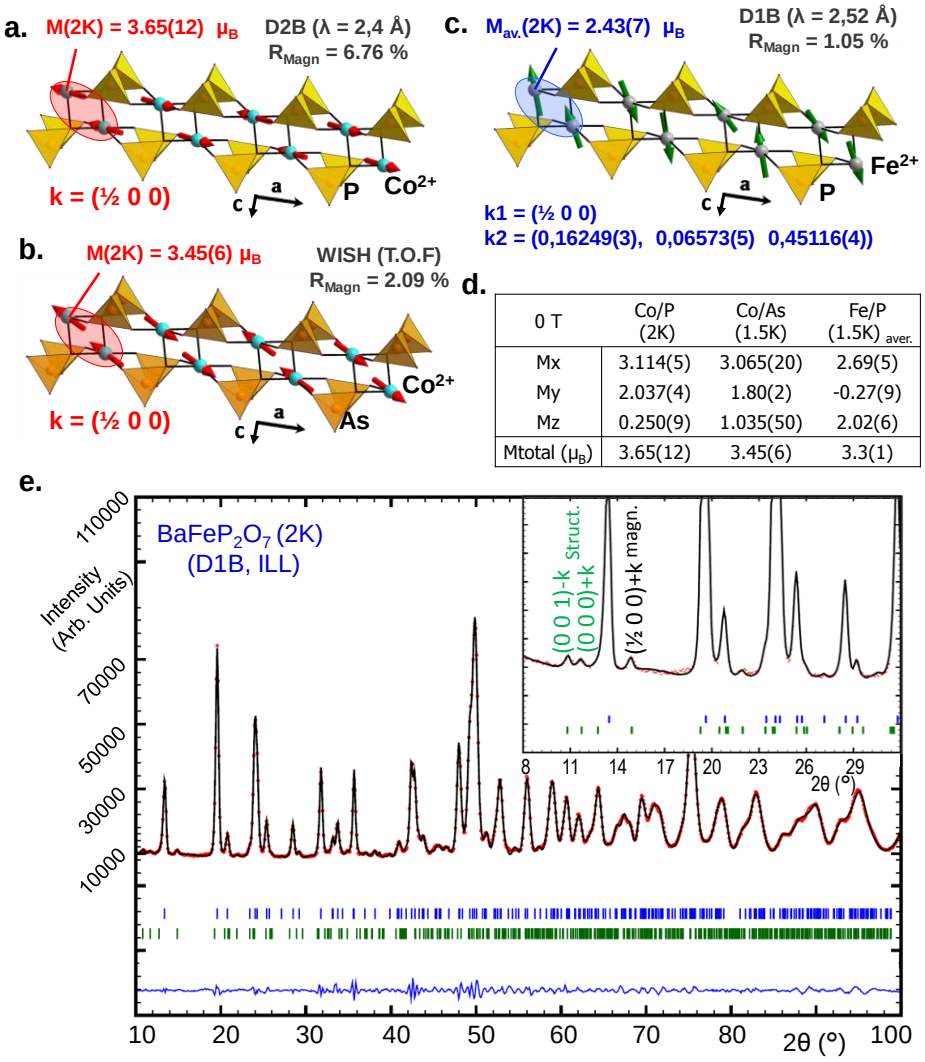

0 T	Co/P (2K)	Co/As (1.5K)	Fe/P (1.5K) aver.
Mx	3.114(5)	3.065(20)	2.69(5)
My	2.037(4)	1.80(2)	-0.27(9)
Mz	0.250(9)	1.035(50)	2.02(6)
Mtotal (μ_B)	3.65(12)	3.45(6)	3.3(1)

Figure 4 | Magnetic Structures: Collinear and modulated spin arrangement for **a)** $BaCoP_2O_7$ **b)** $BaCoAs_2O_7$ **c)** $BaFeP_2O_7$ with refined moment values and k vectors. The FM dimers are highlighted. **d)** Refined Mx, My, Mz components (full and average for Co^{2+} and Fe^{2+} cases respectively). **e)** Exp., calc. and difference NPD patterns for $BaFeP_2O_7$ (see text for details) with evidences of incommensurate structural (green) and magnetic (black) satellites.

$BaCoAs_2O_7$ Magnetic phase diagram: In addition to its counter-intuitive collinear AFM ground state blind to the displacive atomic wave, the atypical $BaCoAs_2O_7$ M(H) dependence deserves attention. It was studied by NPD under magnetic field, using the data shown in Figure 3a. We used a densified $BaCoAs_2O_7$ polycrystalline pellet, *a priori* not sensitive to domains reorientations and tested by collecting data increasing the field from 0 to 8T but also decreasing the field, to verify the recovery of the 1st branch measured intensities. Due to the coexistence of up-to-three magnetically ordred phases, the refinements were performed using the $M_{(2K,\ 0\text{-}8T)} - M_{(20K,\ 0T)}$ difference patterns. Under field, only PND data of the $BaCoAs_2O_7$ phase have been exploited due to a high ratio of moisture and high background collected in the phosphate case, see the Supplementary materials So. Dealing with NPD under field, the following quantitative results should be considered with precaution due to the

formation of purely magnetic textures of orientational character along the magnetic field. In the metamagnetic $BaCoAs_2O_7$, because the field-induced phases appear at the expense of the AFM ground state for specific relative "*spin vs. field orientations* ", the refinements under field were conducted with respect to : i) the conservation of the sums of the scaling factors with respect to the value refined at 0 T, in order to probe the same amount of spins at each stage. ii) the use for all phases of "magnetic" preferred orientation along the easy axis, *i.e* the AFM spin direction [301], in order to model the changing contribution of these domains along with the phase transformations. The Figure 5a displays parts of the difference pattern at 1.5 K recorded for H = 0, 5.5 and 8 T. The refined results for these fields values are summarised in Figure 5e.

Spin-density-Wave under field: For $BaCoAs_2O_7$ above H= 2 T, incommensurate magnetic reflections locked on the k = q = [0.13571(4), 0.07806(5), 0.47683(5)] structural q-vector start growing, more intense at high field, see Figure 5a indexed as (1 1 0)–q (0 1 0)–q. Here the Co^{2+} moment of the AFM phase determined at 1.5 K being very close to the one refined using the full pattern (μ_{Co} = 3.35(8) μ_B versus M = 3.45(6) μ_B, close to the experimental M_{14T} value of 3.4 $\mu_{B/Co}$, it was fixed for the AFM contribution during our refinements of the 5.5 T and 8 T NPD data. The modulated magnetic structure corresponds to an incommensurate spin density wave (SDW) with the spins almost confined in the *bc* plane. Our refinement give the variation of the local moments between 0 and *ca.* 1.9 μ_B nearly perpendicular to their orientation in the Néel ordered state, see Figure 5a,c. This amplitude and direction were fixed equal at 5.5 and 8 T. The resulting refined massic ratios are given in the Figure 5e. Topologically, this SDW is similar to the magnetic structure observed in the quasi-one-dimensional Ising-like $(Ba,Sr)Co_2V_2O_8$ which experimentally also shows a brutal phase transition into a Tomonaga-Luttinger liquid with SDW [12,37].

Ferromagnetic state: Above 7 T, the ferromagnetic contribution appear, mainly observed on the (0 1 0) and (0 0 1) reflexions, (see Figure 5d). According to a spin flip scenario, the AFM and FM phases were constrained to have the same moments, without penalisation of the reliability factors. This is also in agreement with the single crystal magnetisation superior along the a and b-axes in agreement with easy magnetic axis mainly along the *a* direction (see Figure 2a).

Although the refined ratio should be considered with much precaution, they picture that the AFM phase is destabilised by the magnetic field and reduces its amount from 100 % (0 T) to 74 % (5.5 T) to 49 % (8 T), see Figure 5e. The SDW and FM phases appear at the expense of the AFM one, as shown in Figure 5a. Further assumptions require single crystal data, but a plausible scenario can be proposed, taking into account the easiest softening of the Néel ordering with H along the AFM spin direction, as confirmed by single crystal magnetization, see Figure 2a. Then, using a densified polycrystalline sample, the evolution of the three phases roughly respects the distribution of the domains towards the external field. The FM state (23 %) at 8 T is far from the expected amount observed from magnetization which suggests a strong contribution of disordered moments in a forced aligned state and suggest that

the spins reversal occur preferentially for the grains with spins parallel to H as expected for a spin flip, while transversal ones preserve the AFM ordering. The SDW then appears as minimal energy option in the intermediate orientations. A synopsis of the behaviour under magnetic field is proposed in the Supplementary Figure 4e.

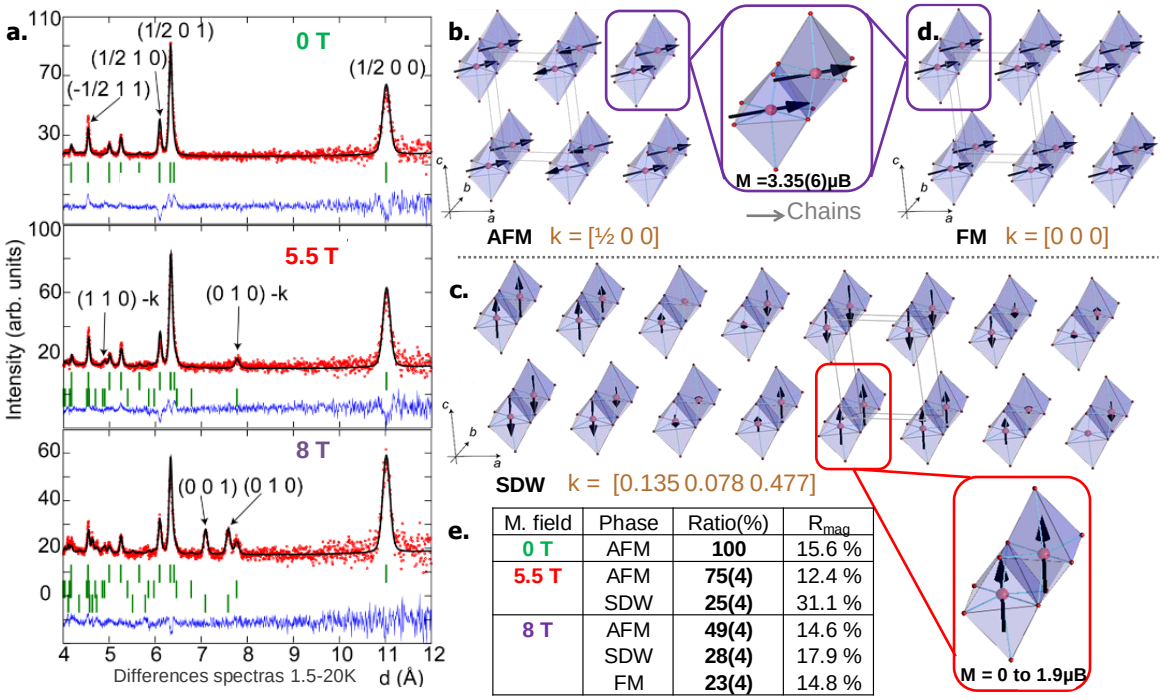

M. field	Phase	Ratio(%)	R_{mag}
0 T	AFM	**100**	15.6 %
5.5 T	AFM	**75(4)**	12.4 %
	SDW	**25(4)**	31.1 %
8 T	AFM	**49(4)**	14.6 %
	SDW	**28(4)**	17.9 %
	FM	**23(4)**	14.8 %

Figure 5 | $BaCoAs_2O_7$ Magnetic structure under magnetic field: a) 1.5 K – 20 K PND difference patterns at H = 0, 5.5 and 8 T and Rietveld refinement profiles using time-of-flight NPD WISH from the bank centred at 58 °. Only the AFM phase is present at H = 0 T. AFM and SDW phases coexist at 5.5 T. AFM, SDW and FM phases coexist at H = 8 T. **b-d)** Magnetic structures of the variants under field with insets pointing out the FM dimers. **e)** Resume of the refined fraction and $R_{magn.}$ for each phases versus the applied field.

Metamagnetic Transitions of modulated origin: The main magnetic exchanges calculated for the average cells are listed in the Table 1. Considering highly correlated 3*d* electrons we used GGA+U (U = 4 for Co^{2+} and 6 eV for Fe^{2+} [18,20,38]) and the taken magnetic configurations are those preliminary used for $BaCoAs_2O_7$ [21], see Supplementary Figure 5 for details (representation of the ordered spin states, values of geometrical parameters along the magnetic exchanges paths, and resulting values of magnetic exchanges parameters). J_{dimer} are systematically found ferromagnetic correspondingly to the refined magnetic structures. J_{chain} corresponds to the strongest exchange between two dimers ($J_{dimer}/k_b = 7.5$ K) along the chains and is AFM with sizeable values well correlated to the θ_{CW} temperatures. J_c corresponds to the interchain coupling in the (*ac)* plane but was estimated neglectable for $BaCoAs_2O_7$ in the average cell (J_c = - 0.8 K). Similarly, no orbital overlap contributes to the exchange along *b* (J_b), suggesting a very weak value also, which gives a pronounced 1D topology to the average systems. Although variable intra/inter values between the compounds, the J_{dimer}/J_{chain} ratio remain close (see Table. 1, and Supplementary Table 5 for details) leading to similar T_N ~10 K in the full series. Here, the undulated atomic strings are necessary tools to bring the frustration into a

pseudo-2D topology necessary for an abrupt reversal of the spins under magnetic field in $BaCoX_2O_7$ as suggested in our prior work [21]. We have used Quantum Monte Carlo (QMC) simulations of M(H) evolution for $BaCoAs_2O_7$ to validate the modulation role, using both the "*average*" and a "*modulated-approximated*" periodic models. The QMC modelization was performed taking Ising S = 3 macro-spins to model Co^{2+} FM pairs. Details of the calculations are given in Supplementary Figure 5.

For the *average* model the QMC-calculated M(H) plot is shown in the Figure 6c, using magnetic exchanges already presented in Table 1, *i.e.* J_{chain}/k_B= -7.5 K, J_c = -0.8 K. For the 3-D connection, along the b-axis we assumed $J_b = J_c$, see Figure 6a. Qualitatively, our quasi-1D "average model" does not reproduce neither the low-field magnetization which experimentally remain unchanged nor the metamagnetic step observed above 5 T in $BaCoX_2O_7$. However, we calculated a broad flat anomaly at Ms/2 around 6 T most plausibly assigned to ferrimagnetic metastable states similar to what calculated by QMC for the 1-D $Ca_3Co_2O_6$ compound [39]. Summarizing, it is clear that the average model lacks a pronounced frustrated character to reproduce the abrupt M(H) step. Indeed, the intensively studied 1/3 magnetization step is theoretically promoted by next-nearest neighbour (NNN) frustration in 1D-isotropic quantum spin chains [40] or by a certain degree of frustration in 2D triangular lattices[41].

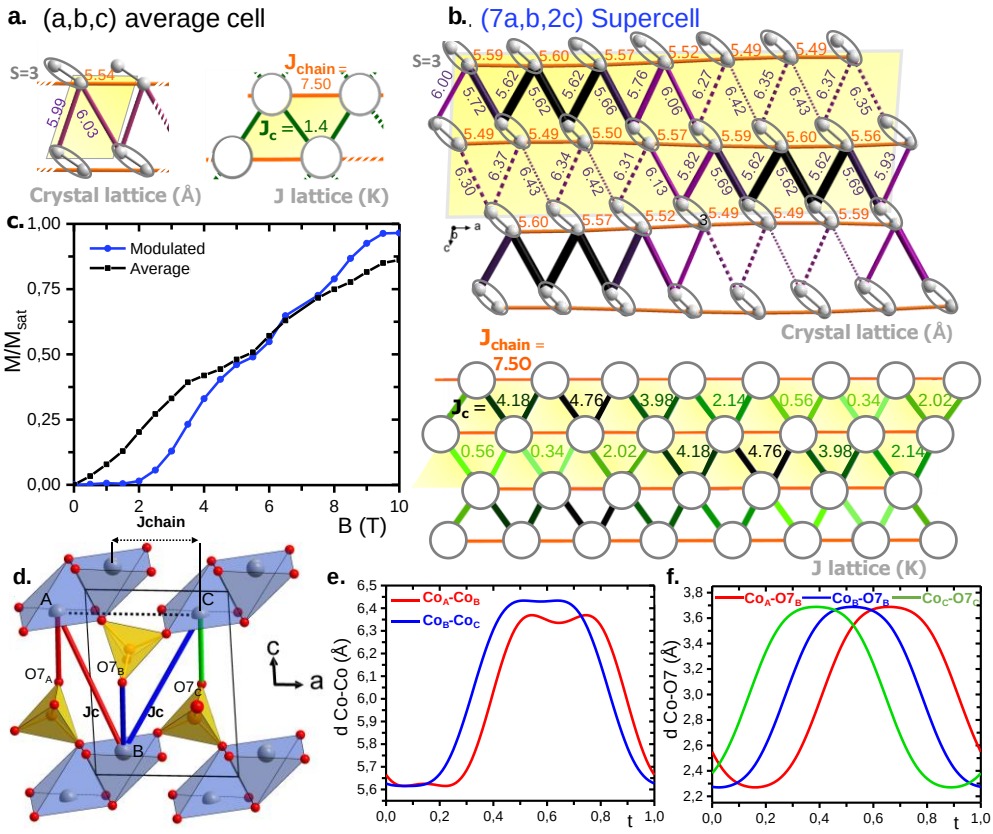

Figure 6 | QMC simulations: a) average crystal structure: atom (left, d in Å) and exchange (right, J/k_b in K) used for the QMC M(H) simulation using S=3 Ising spins for the FM dimers. The perpendicular J_b= -0.8K value is weak. **b)** 7a,b,2c approximant for the incommensurate structure with the atom (top) and exchange lattices. J_{chain}= 7.5 and J_b= -0.8K are taken constant. **c)** QMC M(H) calculations for the two models with the abrupt metamagnetic transition appearing in the pseudo-modulated lattice only. **d, e, f)** validation of the two equivalent J_c values approximation for each J_{chain}-J_c-J_c triangle plotting the

involved Co-Co and Co-O distances which evolve closely in the crystal along the t-modulated real space axis. The bond color of d) are used in e-f) plots.

For the "*incommensurate*" modelization, the $BaCoAs_2O_7$ modulated lattice with q = (0.13571(4), 0.07806(5), 0.47683(5)) was approximated in a 7*a* x *b* x 2*c* superlattice to approach the real 2D incommensurate distribution of exchanges, see Figure 6b. Despite severe undulation of the chains along the c-axis the topology along the chain-axis (a-axis) remains approximately constant, which results in a unique J_{chain} exchange of -7.5 K for simplification, see Figure 1. The complex distribution of exchanges in the (*ac*) plane was estimated using four local structures found in the crystal, at t = 0.15, 0.40, 0.65, 0.90, see Figure 1c,where the real space coordinate was previously defined. They cover the full range of interchain Co-Co distances. For each local structure, J_c was calculated by DFT, plotted against the Co-Co distance and fitted by a linear $J(d_{Co-Co})$ dependence, see Supplementary Figure 5. Finally, after building the 7*a* x *b* x 2*c* approximant structure each i^{th} interchain Co-Co, distance was converted in a specific $J_{c,i}$ value, leading to the super lattice shown in the Figure 6b. Here again, we assume two equivalent exchanges per frustrated J_{chain}, J_c, J_c triangle. The validity of this additional approximation is verified plotting the two d(Co-Co) concerned distances that evolve closely in the real space axis, see the Figures 6d,e,f. Also the three Co-O7 bonds mediating the Co-O7-O7-Co superexchange paths, show very similar evolutions which comforts the validity of two nearly J_c values in each $(S=3 \text{ dimer})_3$ triangle.

The calculated magnetization is shown in the Figure 6c, with evidence of a constant magnetization at low field followed by an abrupt step at 2.5 T (smaller than the exeperimental 5 T critical field). This calculated metamagnetic state validates the importance of the frustrated areas in the (*ac*) plane created by the undulation of the chains. According to our "*Ising model*" QMC procedure, it represents the setting of spin-flipping that initiates the spin reversal until saturation. Similarly, to our "*average*" simulation, the QMC anomaly calculated at M(H)/2 most possibly represents metastable states offered in the model. At least, although severe approximations, the Figure 6b allows visualizing the distribution of Js in $BaCoX_2O_7$ and questions about the rather simple magnetic structure (k = ½ 0 0) previously reported.

Multiferroicity: Group theory analysis using Isosubgroup [34,35] shows that the experimental GP1|mX1+ irreducible representations is compatible with two magnetic space groups P11'_c(a,b,g)00 and P-11'_c(a,b,g)00, not distinguishable using NPD due to weak atomic displacements after spin-lattice coupling. The former allows spin-driven multiferroicity fulfilling a nonpolar/polar symmetry break, see Supplementary Table. 6.

It was checked measuring the dielectric constant ε of $BaCoAs_2O_7$ across the AFM transition under applied magnetic fields. Using a single crystal 300 x 40 x 20 μm^3 with contacts mounted along the a-axis, *i.e.* the chain direction, ε(T) deviates from linearity below T_N and drastically drops below 7K. the magnetocapacitance is significant at low temperature (see Figure 7a). The needle-like shape-factor (e/S) of this crystal being problematic for accurate dielectric measurements (ε=Cp x e/S) we

show the relative dielectric constant across T_N, defined as $\varepsilon/\varepsilon_{20K}$. A dense pellet was also used, also showing a sensitive divergence of the dielectric constant $\varepsilon(T)$ below T_N and clear magneto-electric coupling at 9 T, Figure 7b, see also Supplementary Figure 9. A similar $\varepsilon(T)$ drift was reported for the $CoCr_2O_4$ spinel below 27 K where the material develops concomitantly a spiral magnetic structure and polarization[42]. Polycrystalline pellet and single crystal samples display contrasted deviation from the high temperature interpolation around T_N. However, in the former sample, dC/dT precisely locates the anomaly at T_N proving a weak but clear ME coupling. Remarkably, the thermal evolution of ε for polycrystalline $BaFeP_2O_7$ refutes any ME coupling in this compound, see Figure 7b. It was also checked at 10 K that no significant magnetodielectric effects occur, see Supplementary Figure 6, which suggests the decisive role of the spin orientation and collinearity in these series.

For $BaCoAs_2O_7$, the magnetodielectric profiles collected below T_N, see Figure 7c, highlights a sharp increase of ε even at low magnetic fields, and are symmetric at all temperatures. The magnitude of the magnetodielectric response MD defined as $[\varepsilon_{(H)} - \varepsilon_{(H=0)}]/\varepsilon_{(H=0)}$ increases by a factor of ~2 from 10 K (just below T_N) to 7 K, and proves ME effects. It reaches 0.03 % at 9 T, similar to what observed in the multiferroic $NiCr_2O_4$[42,43]. It could reasonnably well be fitted using linear ME couplings, but the 7 K and 8 K data also show a sensitive break above H = 4-5 T, above the critical field for the metamagnetic field. Keeping in mind that at 2 K NPD suggests the appearing of the SDW phase and FM-ordered phase above 2 and 5.5 T respectively, see the Figure 5, the strictive effect due to forced-alignement of disordred spin component is plausible.

The electric polarization was evaluated by measuring the pyroelectric current on both polycrystalline and single crystal $BaCoAs_2O_7$. Using the pellet, leakage currents were too large for a safe poling. Using cut piece of single crystal with contacts along the [100] direction, after poling at 30 K down to 6 K under +50 V a pyrocurrent is developed below T_N. An electrical polarization of ~250 $\mu C/m^2$ is estimated at 6 K as shown in the Figure 7d which comfort the setting of spin-induced polarization out of the centrosymmetric P-1(α,β,γ)0 4D super space group at room temperature. The polarization magnitude should be taken carefully due to the approximative geometrical factor used and non homogeneous edge effects of electric field. The anomaly detected below 7K is consistent with the $\varepsilon(T)$ drop noted in the Figure 7a, but was not identified magnetically nor structurally at the moment. Ferroelectricity implies the existence of a spontaneous polarization, leading the pyrolectric current, which direction can be fully switched by a sign change of the electric field. Here, the polarization was partially returned after -50 V poling, due to inherent difficulties to reverse ferrolectric domains in a single crystalline sample.

All together the co-presence of switchable spin-induced polarization and magneto-electric couplings below T_N validate the realization of type II multiferroricity, of particular origin. Especially, besides most identified mechanisms for type-II multiferroicity, including the Dzyaloshinsky Moriya inverse (DMI) effect for which a periodic structure with modulated spin structure breaks the space symmetry, $BaCoX_2O_7$ compounds imply a paradoxal situation, where a structurally modulated centrosymmetric lattice together with commensurate collinear spin order develops multiferroicity, see the Figures

8a,b. On the opposite, magnetoelectric measurements on a $BaFeP_2O_7$ pellet of similar quality, does not show any detectable magnetoelectric effects, see the inset of the Figure 7a and Supplementary Figure 6.

Discussion: Dealing with a collinear spin structure in $BaCoX_2O_7$, the polarization induced between two spins *i* and *j* by DMI effect expressed as $P \propto S_i \times S_j$ is based on SOC but cannot prevail in our compounds, leading to null local terms. The second refutable mechanism is the spin-dependent hybridization model (spin-charge coupling), mediated by the spin-orbit interaction. It is based on the variation of the ionic charge of the oxygen depending on the angle between the spin and the metal-oxygen bond, able to generate polarization in absence of atomic shift. According to this mechanism the local polarization of the CoO_{5+1} polyhedra is expressed by $P \propto \sum_{i=1}^{5-6}(S.e_i)^2 e_i$ where e_i is the unit vector along the i^{th} Co- bond. This mechanism, was first reported for 120 ° spin structure delafossite [44,45], and also identified in $Ba_2CoGe_2O_7$ with obvious chemical [46] resemblances dealing with the $BaO\text{-}CoO\text{-}X_2O_5$ chemical system. However, in $BaCoAs_2O_7$ the spins are lying in the O_4 square plane, while in-plane polarization should be cancelled by opposite bonds for a CoO_4 ideal square plane. Although the Co^{2+} centered polyhedra is significant distorted in plane, its 4D-centrosymmetric distribution and elongation with regard to the *P-1(α,β,γ)0* superspace group refutes any significant polarization along the chain axis.

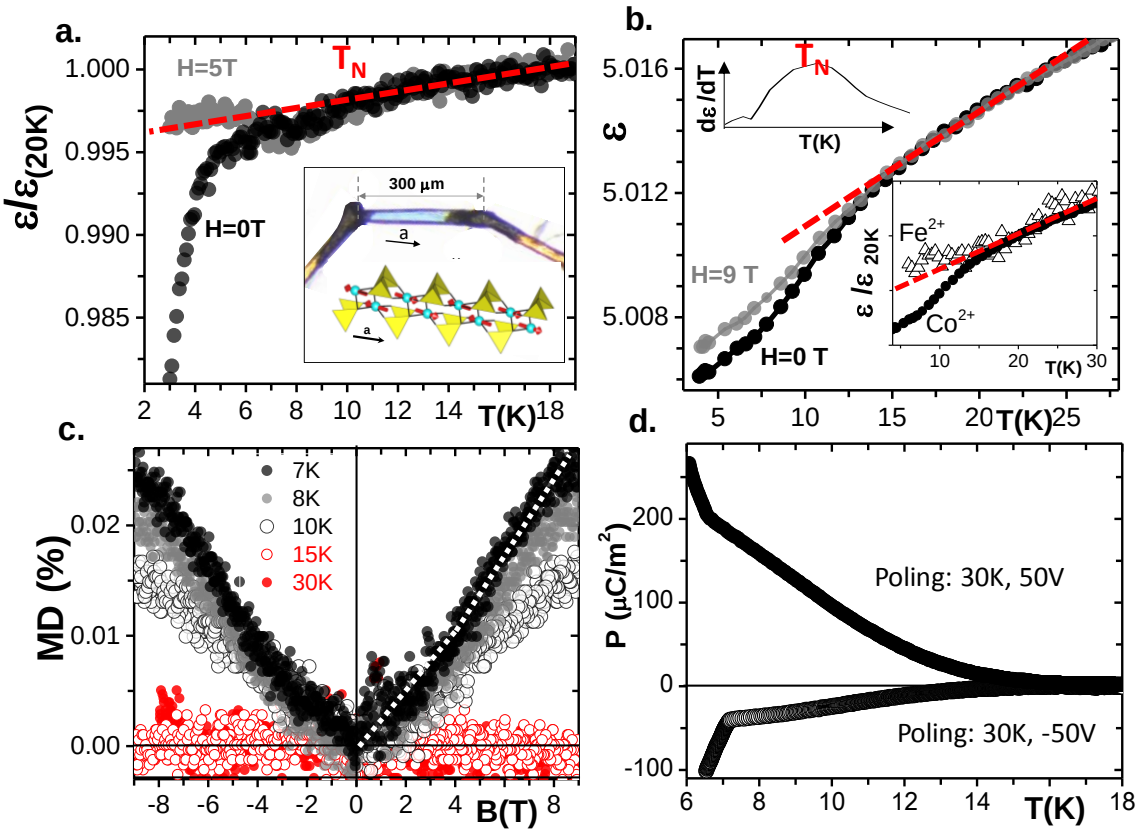

Figure 7 | Magnetoelectric properties a) relative dielectric constant at H=0 and 5T for a $BaCoAs_2O_7$ needle shaped crystal. **b)** similar measurement at 0 and 9T on dense pellet. The inset shows no thermal dependence of the relative ε for $BaFeP_2O_7$ **c)** Magneto dieletric (MD) profiles at various temperature. The white broken line is a guide for the eye. **d)** Pyroelectric measurement (poling) performed on $BaCoAs_2O_7$ single crystal, with evidence of polarity below T_N.

Then, the third proposed mechanism concerns the exchange-striction proposed in antiferromagnetic collinear systems, such as the Ising chain Ca_3CoMnO_6[22]. This mechanism relies on the loss of spatial symmetry in specific ↑↑↓↓ magnetic units, scaled by the inner $S_i.S_j$ scalar product within a direct spin-lattice coupling, blind to the particular directions of magnetic moments. In the AFM chains of S = 3 dimers, this mechanism is cancelled and not discriminant between the spin-collinear Co^{2+} but spin-modulated Fe^{2+} compounds. Finally no clear scenario emerges, complicated by incommensurate structural topology. It is uncertain to assess if the collinear structure found for Co^{2+} compound is a necessary ingredient for multiferroicity. Indeed it was verified by group theory analysis [34,35] that similarly to the inversion-breaking allowed for $BaCoX_2O_7$ after spin-lattice coupling, it is also allowed for $BaFeP_2O_7$ after coupling the modulated superspace group with the two magnetically active k vectors (½ 0 0 and αβγ) in the polar subgroup $P1(a,b,g)0$.
Therefore searching for contrasted argument for the paraelectric to ferroelectric destabilization for the multiferroic Co^{2+} materials compared with the ME-inert Fe^{2+} may rely on the spin orientations via magnetic dipole dipole (MDD) interactions. These nanoscale forces are known to have significant effects self-assembly of magnetic particles [47], but can also play a decisive role in the orientations of spins in bulk-magnetic structures when surpassing antagonist SOC effects, see for instance $Sr_3Fe_2O_5$[48], MAs_2O_6 (M = Mn, Co, Ni) [49], $Mn_4Ta_2O_9$[50]. We argued in the $BaMX_2O_7$ series that the sizeable SOC drives the moments nearly in-(*ab*) plane (Co^{2+} compounds) versus perpendicular to the chains (Fe^{2+} compound) and one may propose the MDD as destabilizing ingredients in the multiferroic cases. The m_j to m_k MDD interaction is given by:

$$MDD : H = -\left(\frac{{\mu_B}^2}{{a_0}^3}\right)\left(\frac{a_0}{r_{jk}}\right)^3 \left[3(m_j.e_{jk})(m_k.e_{jk}) - m_j.m_k\right]$$

Where $m_{j,k}$ are refined moments in μ_B, a_o is the Bohr radius (0.529 177 Å, r_{jk} is the distance between the spin sites j and k, and e_{jk} is the unit vector along the inter-site distance. (μ_B^2/a_o^3) = 0.181 meV.

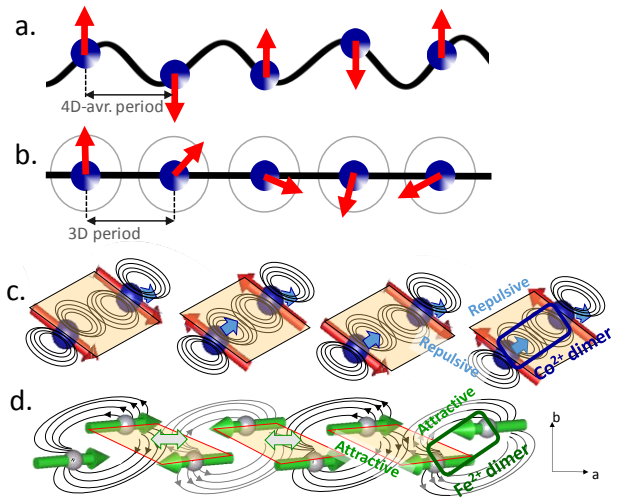

Figure 8 | Proposed ME mechanism: paradox between **a)** the incommensurate modulated atomic string with collinear spins and **b)** the modulated spin structure over a 3D lattice (IDM case) **c)** repulsive vs **d)** attractive dipole-dipole magn. Interaction in Co^{2+} (with possible atomic shift shown by blue arrows) against Fe^{2+} compounds

We summed up all of the MDD terms whose distances r_{ij} are shorter than a cutoff distance r_c = 10.5 Å (see Supplementary Tables 7) after which contributions were neglectable using the refined average moment vectors in the Fe case. We found destabilizing (positive) and stabilizing energies for $BaCoX_2O_7$ (+14.48 10^{-3} meV for As and +23.76 10^{-3} meV for P, per Co site) and $BaFeP_2O_7$ (-2.88 10^{-3} meV per Fe site) respectively and MDD could be a driving force to develop the experimental spin-induced polarity. In addition the intra-dimer dipolar interactions ($J_{dd\ dimer}$) and inter-dimer between two next metal sites ($J_{dd\ chain}$) give both repulsive interactions in $BaCoX_2O_7$ compounds against both attractive ones in $BaFeP_2O_7$ due to the spin orientations, see the Figures 8c,d. The calculated J_{dd} interactions are given Table 1 and detailled in Supplementary Tables 7 for all counted neighbors. Athough weaker, one notes the same order of magnitude of Jdd's compared to the through-bond J exchanges which denote significant through-space effects.

While the destabilization into a polar mode of the crystal structure by MDD couplings appear vain in a regular lattice due to next-neighbor cancellation, dipole-dipole ordering was recently proposed to explain magnetolectric anomaly at the setting of low-D ordering in 1-D materials [51]. Practically, dealing with aperiodic materials, infinite periodicities within structural chains, versatile Co^{2+} local coordinations along them, and their slicing by local defects, the destabilization by cooperative repulsive striction effects may be proposed to generate a polar mode. Even if cooperative, atomic displacements in one chain are not expected regular and should be shifted between chains due to the 3D-structural modulation giving to each Co-site local specificities. Therefore, one can imagine a polar mode mechanism relaxing the MDD stress from chain-to chain.In opposite the energetic stabilization of $BaFeP_2O_7$ by MDD would preserve the spatial inversion from site to site, in good agreement with the attractive interactions along the chains which cancel from site to site.

Besides the proposition of a novel type II multiferroic series of materials, the possibility for an original mechanism for spin-induced polorization by mixing several ingredients such as the SOC influence into uniaxial spin structure, incommensurate atomic strings and well adapted dipole-dipole interaction offers a new paradigm in this field. The aperiodic lattice contribution to magneto-electric exchanges was already proposed in Cr-doped multiferroic $BiFeO_3$[52], but more generally our results open wide perspectives about the screening of incommensurate modulated materials so far not considered as multiferroics due to the identified conventional mechanisms.

ASSOCIATED CONTENT

Supporting Information guidelines

The supporting information is available free of charge on the …. Website at DOI: ……

The files (PDF) gives detailed information related to the structural and single crystal refinement for $BaFeP_2O_7$, additional specific heat plots, extra-crystallographic details and magnetic plots for Fe/Co mixed compounds, details related to magnetic structures and NPD refinement (such as refinement of $BaFeP_2O_7$ structure in a non-modulated magnetic case), details for DFT calculations, magnetoelectrics couplings, magnetic dipole-dipole calculations, SEM-EDS analysis, spectroscopies measurements, and lastly additional information related to TGA measurement and proofs of significant moisture in "non-fresh" cobalt compounds. This file contains 26 pages, 9 parts, 14 figures and 16 Tables.

One can find X-Ray crystallographic data for $BaFeP_2O_7$ average + modulated structures CSD 1996565 and the related Check-cif report (PDF).

AUTHORS INFORMATION

Corresponding Author.
*olivier.mentre@univ-lille.fr

ORCID
Bastien Leclercq : 0000-0002-3165-322237
Angel M. Arevalo-Lopez : 0000-0002-8745-4990
Houria Kabbour : 0000-0002-9081-3261
Claire V. Colin : 0000-0003-1332-7929
Sylvie Daviero-Minaud : 0000-0003-3887-5585
Alain Pautrat :
Tathamay Basu : 0000-0002-8486-189X
Ranjana-Rani Das : 0000-0002-9781-3432
Vaclav Petricek: 0000-0002-9731-8730
Rénald David :
Olivier Mentré : 0000-0002-1822-6003

Notes
The authors declare no competing financial interest.

ACKNOWLEDGMENT

This work was carried out under the framework of the LOVE-ME project supported by the ANR (Grant ANR ANR-16-CE08-0023). AMAL thanks a Marie-Słodowska Individual Fellowship in the Horizon 2020 research and innovation programme under grant agreement 750971 ("KISS ME"). The Fonds Européen de Développement Régional (FEDER), CNRS, Région Hauts-de-France and Ministère de l'Education

Nationale, de l'Enseignement Supérieur et de la Recherche are acknowledged for funding of the PPMS and the X-ray diffractometers.. Chevreul Institute (FR 2638), Ministère de l'Education Nationale, de l'Enseignement Supérieur et de la Recherche, Région Hauts-de-France, FEDER are acknowledged for supporting this work. We also thanks the GDR MEETICC for the funding through the « Soutien aux jeunes chercheurs » supply. We thank Laurence Burylo, Nora Djellal & Claire Minaud at the UCCS for their experimental contribution. We also acknowledge the CRG- D1B, Institut Laue-Langevin at Grenoble, France for beam time allocation and the technical assistance of V. Nassif, S. Djellit. BL, OM and AAL acknowledge Vaclav petricek for his advice refining concomitantely modulated crystal and magnetic structures in absence of magnetic fields.

REFERENCES

[1] T. Hu, E. Kan, *Wiley Interdiscip. Rev. Comput. Mol. Sci.* **2019**, *9*, 1.

[2] S. Dong, J.-M. M. Liu, S.-W. W. Cheong, Z. Ren, *Adv. Phys.* **2015**, *64*, 519.

[3] N. A. Hill, *J. Phys. Chem. B* **2000**, *104*, 6694.

[4] R. Ramesh, S. N. A., *Nat. Mater.* **2007**, *6*, 21.

[5] J. F. Scott, *Phys. Rev. B* **1977**, *16*, 2329.

[6] M. Fiebig, T. Lottermoser, D. Meier, M. Trassin, *Nat. Rev. Mater.* **2016**, *1*, 1.

[7] S. Dong, H. Xiang, E. Dagotto, *Natl. Sci. Rev.* **2019**, *6*, 629.

[8] W. Eerenstein, N. D. Mathur, J. F. Scott, *Nature* **2006**, *442*, 759.

[9] M. Lenertz, A. Dinia, S. Colis, O. Mentré, G. André, F. Porcher, E. Suard, *J. Phys. Chem. C* **2014**, *118*, 13981.

[10] K. Singh, A. Maignan, D. Pelloquin, O. Perez, C. Simon, *J. Mater. Chem.* **2012**, *22*, 6436.

[11] T. Giamarchi, C. Rüegg, O. Tchernyshyov, *Nat. Phys.* **2008**, *4*, 198.

[12] E. Canévet, B. Grenier, M. Klanjšek, C. Berthier, M. Horvatić, V. Simonet, P. Lejay, *Phys. Rev. B* **2013**, *87*, 054408.

[13] B. Leclercq, H. Kabbour, F. Damay, C. V. Colin, A. Pautrat, A. M. Arevalo-Lopez, O. Mentré, *Inorg. Chem.* **2019**, *58*, 12609.

[14] R. David, H. Kabbour, S. Colis, O. Mentré, *Inorg. Chem.* **2013**, *52*, 13742.

[15] L. Bogani, A. Vindigni, R. Sessoli, D. Gatteschi, *J. Mater. Chem.* **2008**, *18*, 4750.

[16] D. Gatteschi, A. Vindigni, in (Eds.: J. Bartolomé, F. Luis, J.F. Fernández), Springer Berlin Heidelberg, Berlin, Heidelberg, **2014**, pp. 191–220.

[17] B. Leclercq, H. Kabbour, A. Arevalo-Lopez, M. Huvé, S. Daviero-Minaud, C. Minaud, I. Blazquez Alcover, O. Mentré, *Inorg. Chem. Front.* **2019**, *7*, 239.

[18] R. David, A. Pautrat, D. Filimonov, H. Kabbour, H. Vezin, M.-H. Whangbo, O. Mentré, *J. Am. Chem. Soc.* **2013**, *135*, 13023.

[19] L. P. Regnault, P. Burlet, J. Rossat-Mignod, *Phys. B+C* **1977**, *86–88*, 660.

[20] H. Kabbour, R. David, A. Pautrat, H. Koo, M. Whangbo, G. André, O. Mentré, *Angew. Chemie Int. Ed.* **2012**, *51*, 11745.

[21] R. David, H. Kabbour, S. Colis, A. Pautrat, E. Suard, O. Mentré, *J. Phys. Chem. C* **2013**, *117*, 18190.

[22] Y. J. Choi, H. T. Yi, S. Lee, Q. Huang, V. Kiryukhin, S. W. Cheong, *Phys. Rev. Lett.* **2008**, *100*, 6.

[23] S. Petit, *Physics (College. Park. Md).* **2013**, *6*, 4.

[24] A. A. Belik, M. Azuma, M. Takano, *Inorg. Chem.* **2005**, *44*, 7523.

[25] D. Riou, H. Leligny, C. Pham, P. Labbe, B. Raveau, *Acta Crystallogr. Sect. B* **1991**, *47*, 608.

[26] A. Moquine, etudes chimique, structural et magnetique de nouveaux mono- et diphosphate apparaissant dans les diagrammes ternaires AO-CuO-P2O5 ; A = Mg , Ca , Sr , *PhD manuscript*, **1990**.

[27] L. Cario, A. Meerschaut, B. Corraze, O. Chauvet, *Mater. Res. Bull.* **2005**, *40*, 125.

[28] V. M. Kovrugin, E. E. Gordon, E. E. Kasapbasi, M. H. Whangbo, M. Colmont, O. I. Siidra, S. Colis, S. V. Krivovichev, O. Mentré, *J. Phys. Chem. C* **2016**, *120*, 1650.

[29] J. Olchowka, M. Colmont, A. Aliev, T. T. Tran, P. S. Halasyamani, H. Hagemann, O. Mentré, *CrystEngComm* **2017**, *19*, 936.

[30] Y. Tsujimoto, Y. Baba, N. Oba, H. Kageyama, T. Fukui, Y. Narumi, K. Kindo, T. Saito, M. Takano, Y. Ajiro, K. Yoshimura, *J. Phys. Soc. Japan* **2007**, *76*, 3.

[31] S. M. Yusuf, A. K. Bera, C. Ritter, Y. Tsujimoto, Y. Ajiro, H. Kageyama, J. P. Attfield, *Phys. Rev. B - Condens. Matter Mater. Phys.* **2011**, *84*, 1.

[32] Z. He, T. Taniyama, T. Kyômen, M. Itoh, *Phys. Rev. B* **2005**, *72*, 172403.

[33] Y. Kawasaki, J. L. Gavilano, L. Keller, J. Schefer, N. B. Christensen, A. Amato, T. Ohno, Y. Kishimoto, Z. He, Y. Ueda, M. Itoh, *Phys. Rev. B* **2011**, *83*, 064421.

[34] B. J. Campbell, H. T. Stokes, D. E. Tanner, D. M. Hatch, *J. Appl. Crystallogr.* **2006**, *39*, 607.

[35] H. T. Stokes, D. M. Hatch, B. J. Campbell, **n.d.**

[36] R. R. Das, C. V. Colin, *Investigating Antiferromagnetic Magnetic Ground State of a Modulated Phase with Metamagnetic Properties of $BaFeP_2O_7$, Institut Laue-Langevin (ILL)*,

[37] A. Okutani, T. Kida, T. Usui, T. Kimura, K. Okunishi, M. Hagiwara, *Phys. Procedia* **2015**, *75*, 779.

[38] A. L. Dalverny, J. S. Filhol, F. Lemoigno, M. L. Doublet, *J. Phys. Chem. C* **2010**, *114*, 21750.

[39] R. Soto, G. Martínez, M. N. Baibich, J. M. Florez, P. Vargas, *Phys. Rev. B* **2009**, *79*, 184422.

[40] A. Honecker, J. Schulenburg, J. Richter, *J. Phys. Condens. Matter* **2004**, *16*, S749.

[41] H. Nishimori, S. Miyashita, *J. Phys. Soc. Japan* **1986**, *55*, 4448.

[42] N. Mufti, A. A. Nugroho, G. R. Blake, T. T. M. Palstra, *J. Phys. Condens. Matter* **2010**, *22*, 075902.

[43] T. D. Sparks, M. C. Kemei, P. T. Barton, R. Seshadri, E. D. Mun, V. S. Zapf, *Phys. Rev. B - Condens. Matter Mater. Phys.* **2014**, *89*, 2.

[44] T. Kimura, *Annu. Rev. Condens. Matter Phys.* **2012**, *3*, 93.

[45] S.-W. Cheong, M. Mostovoy, *Nat. Mater.* **2007**, *6*, 13.

[46] H. Murakawa, Y. Onose, S. Miyahara, N. Furukawa, Y. Tokura, *Phys. Rev. Lett.* **2010**, *105*, 1.

[47] K. J. M. Bishop, C. E. Wilmer, S. Soh, B. A. Grzybowski, *Small* **2009**, *5*, 1600.

[48] H. J. Koo, H. Xiang, C. Lee, M. H. Whangbo, *Inorg. Chem.* **2009**, *48*, 9051.

[49] H. J. Koo, M. H. Whangbo, *Inorg. Chem.* **2014**, *53*, 3812.

[50] N. Narayanan, A. Senyshyn, D. Mikhailova, T. Faske, T. Lu, Z. Liu, B. Weise, H. Ehrenberg, R. A. Mole, W. D. Hutchison, H. Fuess, G. J. McIntyre, Y. Liu, D. Yu, *Phys. Rev. B* **2018**, *94*, 1.

[51] T. Basu, C. Bloyet, J. M. Rueff, V. Caignaert, A. Pautrat, B. Raveau, G. Rogez, P. A. Jaffrès, *J. Mater. Chem. C* **2018**, *6*, 10207.

[52] X. Tang, M. J. Gentiletti, A. Lachgar, V. A. Morozov, B. I. Lazoryak, *Solid State Sci.* **2001**, *3*, 143.

Table of Content

BaCoX2O7 (X=P,As) are shown to be a type II multiferroics based on an original scenario in which incommensurate atomic shifts and collinear AFM ising-spins interact as crucial ingredients. In comparison no magneto-electric coupling was detected in the Heisenberg $BaFeP_2O_7$ isomorph, with strong spin-lattice coupling leading to a modulated AFM spin structure. Magnetic dipole-dipole (MDD) interactions are discreminating between the two systems.